Applied Physics Letters ARTICLE scitation.org/journal/apl

Tuning to more compressible phase in TiZrHfNb high entropy alloy by pressure

Cite as: Appl. Phys. Lett. **116**, 031901 (2020); doi: 10.1063/1.5136022
Submitted: 10 November 2019 · Accepted: 7 January 2020 ·
Published Online: 21 January 2020

Kai Zhang,[1] Shang Peng,[1,2] Nana Li,[1] Xuqiang Liu,[1,3] Mingjian Zhang,[4] Yi-Dong Wu,[5] Yanping Yang,[1] Eran Greenberg,[6] Vitali B. Prakapenka,[6] Xidong Hui,[5] Yandong Wang,[5] and Wenge Yang[1,a)]

AFFILIATIONS

[1]Center for High Pressure Science and Technology Advanced Research (HPSTAR), Shanghai 201203, People's Republic of China
[2]School of Physics and Technology, Center for Electron Microscopy, MOE Key Laboratory of Artificial Micro- and Nano-structures, and Institute for Advanced Studies, Wuhan University, Wuhan 430072, People's Republic of China
[3]Key Laboratory for Anisotropy and Texture of Materials (Ministry of Education), School of Material Science and Engineering, Northeastern University, Shenyang 110819, People's Republic of China
[4]School of Advanced Materials, Peking University, Shenzhen Graduate School, Shenzhen 518055, People's Republic of China
[5]State Key Laboratory for Advanced Metals and Materials, University of Science and Technology Beijing, Beijing 100083, People's Republic of China
[6]Center for Advanced Radiation Sources, University of Chicago, Chicago, Illinois 60637, USA

[a)]**Author to whom correspondence should be addressed:** yangwg@hpstar.ac.cn

ABSTRACT

In this work, the starting nominal $Ti_{25}Zr_{25}Hf_{25}Nb_{25}$ high entropy alloy (HEA) has two body centered cubic (BCC) phases with a volume percentage about 100:1, with the primary phase having a much larger bulk modulus (incompressible) than the uniform single-phase HEA. We found that these two phases merged into one single BCC phase at pressures beyond 36 GPa, whose bulk modulus dropped to that of the normal homogeneous HEA. After decompressing, the new phase can be sustained to ambient conditions. This abnormal pressure-induced softening was largely related to the lattice distortion evolution and interfacial energy during compression.

Over the past decade, a revolutionary alloy design concept, high entropy alloy (HEA) or multi-principal element alloy (MPEA), has attracted much attention with exceptional mechanical and physical properties. The disorder in the atomic configuration usually endows HEA a simple crystal structure to form typical body- or face-centered cubic (BCC or FCC) solid solutions, whose lattice sites are occupied randomly by different sizes and electronic configurations of atoms.[1–7]

Recent research results suggest that the contribution of configurational entropy plays a dominant role in the total Gibbs free energy only within a single-phase system that is close to an ideal solid solution.[8] There are only several limited systems showing a single-phase structure.[9,10] In actual alloys, enthalpy and non-configurational entropy have a great effect on the phase formation of HEA.[8] Therefore, most as-cast HEAs contain precipitations after the solidification process,[11] which largely affects the mechanical properties of HEA.[12,13] In the recent development of metastable dual-phase HEA, which is designed to increase HEAs' strength and ductility through interfacial engineering, the second (minor) phase played an important role in the overall properties of HEA.[5,14] Enhanced strength and ductility in a high-entropy alloy via elaborating ordered oxygen complexes were achieved in TiZrHfNb HEA.[6] However, some brittle precipitated phase may have a detrimental effect on the high temperature application of HEA.[15] In terms of chemical composition, these precipitations show minor composition fluctuation from the matrix phase, even with the similar lattice parameters,[15] which results in strong lattice distortion at the phase boundary.[4,11] The lattice mismatch and interface stress impede the sliding of dislocation and thus generate a higher strength and hardness in HEA.[1] Especially for those HEAs containing Al, the relatively severe lattice distortion was frequently discussed due to the differences in both atomic sizes and interactions between Al and transition metals.[16,17] Despite the fundamental importance of lattice distortion in the mechanical properties and sluggish dynamic behavior of HEA, however, a thorough assessment is still under debate.[18–21] Lattice distortion has been characterized using various tools including X-ray diffraction (XRD),[22] high resolution transmission electron microscopy (HRTEM),[23] Neutron diffraction,[24] x-ray total scattering,

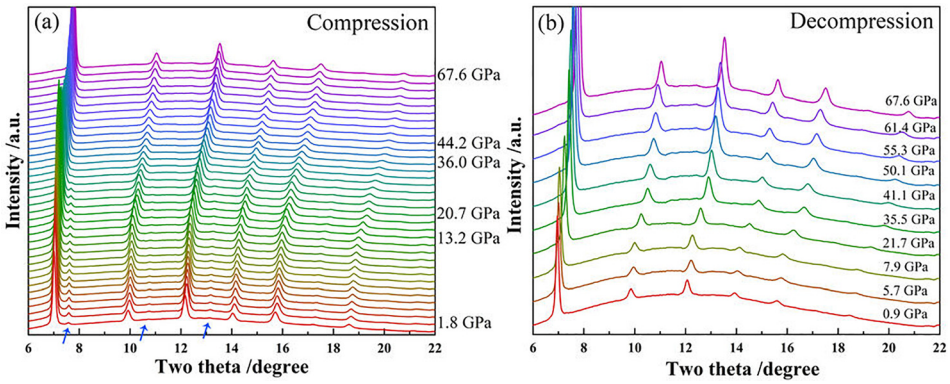

FIG. 1. Compression and decompression studies of TiZrHfNb high entropy alloy under high pressure with synchrotron XRD. XRD profiles during the compression to 67.6 GPa (a) and decompression to 0.9 GPa (b).

and extended x-ray absorption fine structure[19] but yet to be fully understood.

High pressure as a powerful tool can alter the interatomic distance or even electronic configuration and bonding patterns in various materials.[25,26] Recently, a hexagonal close-packed (HCP) phase in CrMnFeCoNi HEA was predicted and synthesized from the FCC structure under high pressure at room temperature.[27,28] It was suggested that FCC-to-HCP phase transition was associated with the suppression of the local magnetic moment.[29] These studies demonstrate that the lattice structure of HEA can be significantly tuned by high pressure at the atomic level, which opens an additional avenue to prepare the dual-phase FCC/HCP high entropy alloy.[5] In this work, we focus on the mechanical response of minor composition variation in HEA during *in situ* compression and decompression and discover that the starting material has much higher bulk modulus (harder to compress) than that in uniform HEA due to the high internal interface strain coexisting with the minor phase. Pressure induced softening transition tunes the mixture phase into the normal uniform HEA. This explains the origin of superior mechanical properties in HEA and the importance of lattice distortion under high pressure.

Compared to 3d transition metal CoCrFeMnNi HEA,[9] the lattice distortion in the refractory TiZrHfNb HEA is much more significant,[24,30] which is a good model to investigate the lattice distortion evolution under high pressure. The prototypical TiZrHfNb BCC-type HEA reaches remarkable lattice distortion up to 2.39% among all known HEAs[22] and shows exceptional structure stability up to 50.8 GPa without phase transition.[31] In our work, *in situ* high pressure XRD measurements were conducted up to 67.6 GPa in compression and back to ambient pressure in decompression as shown in Fig. 1. Material preparation and experimental methods are described in the supplementary material. It is clear that there are two phases at the initial pressure: the main phase and the minor phase with the approximate volume ratio of about 100:1 based on the ratio of peak intensity. The blue arrows in Fig. 1(a) indicate the diffraction peaks from the minor phase. Figure 2 displays the XRD profiles and their Rietveld refinements of the main phase and minor phase by using the BCC structure model at the initial pressure of 1.8 GPa and after decompression at 0.9 GPa, respectively. Due to the weak diffraction intensity of the minor phase (about 1% volumetric percentage), only three peaks from (200), (220), and (311) diffraction planes of the BCC structure can be identified as indicated by the red arrows in Fig. 2. Upon compression, all peaks shifted to the higher diffraction angle side as both unit cells were compressed as shown in Figs. 1(a) and 1(b). Under higher pressures, the diffraction peaks of the minor phase gradually diminished and eventually disappeared at 30.3 GPa. After that, HEA remained in the single BCC phase up to 67.6 GPa, the highest pressure in this work. Upon decompression back to 0.9 GPa, there was not any sign of the minor phase as shown in Fig. 1(b). These results suggest that a uniform HEA can be formed with the aid of high pressure.

As shown in Fig. S1, with the aid of scanning electron microscopy (SEM)-energy dispersive spectroscopy (EDS) analysis, the as-cast sample clearly showed the uniform composition distribution with no formation of large segregation or precipitate at the length scale of this image, and EDS indicates that HEA has nearly an equiatomic composition within the resolution of SEM-EDS. To check the distribution of the minor phase from the as-cast sample, we conducted microstructure analysis using transmission electron microscopy (TEM). The selected area electron diffraction (SAED) pattern along the [111] zone axis shows clear evidence of the co-existence of two BCC structures with different lattice constants [Fig. S2(a)]. The d-spacing values measured from SAED are $d_{110m} = 2.270$ Å, $d_{211m} = 1.311$ Å and $d_{110M} = 2.427$ Å,

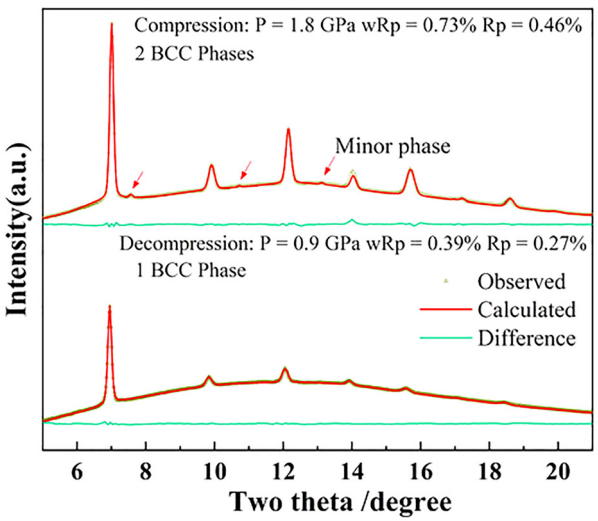

FIG. 2. Rietveld refinements on the XRD profiles at the initial pressure of 1.8 GPa and the decompressed pressure of 0.9 GPa.

d_{211M} = 1.399 Å for minor (m) and main (M) phases, respectively. This is consistent with the d-spacing values from XRD at 1.8 GPa, d_{110m} = 2.234 Å, d_{211m} = 1.290 Å, and d_{110M} = 2.413 Å, d_{211M} = 1.393 Å for minor and main phases, respectively. The difference in lattice constants between these two phases is about 6.5%. The bright field diffraction contrast image [Fig. S2(b)] shows strong strain field distribution around the minor phase nanoparticles. As the particle size of the minor phase (ranged from 10 to 100 nm) is smaller than the SEM-EDS resolution, it is impossible to distinguish the composition variation between these two phases, which explains the "uniform" composition distribution from the EDS map mentioned above.

The XRD peak positions reflect the changes in the unit cell volume during compression/decompression directly. The volume vs pressure relationship was fitted in terms of the third-order Birch–Murnaghan equation of state (B-M EOS).[32] First, from Fig. 3(a), we can see that the unit cell volume of the main phase shows two distinct compression curves (dashed lines) with a distinguishing pressure point at around 23.7 GPa, here, naming them as the low pressure phase

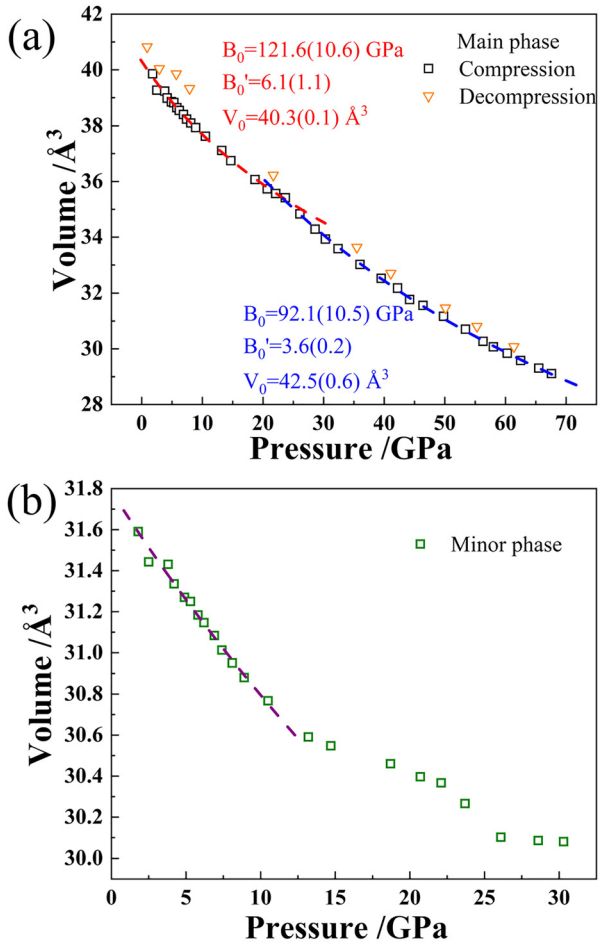

FIG. 3. Unit cell volumes vs pressure for the main phase (a) and the Birch–Murnaghan EOS fitting, the minor phase (b). The dashed lines in (a) are the EOS fitting results from compression data. The dashed line in (b) is just a guide for the eye.

and the high pressure phase, respectively. Separated EOS fittings were conducted for the low pressure phase (1.8–23.7 GPa) and the high pressure phase (23.7–67.6 GPa), respectively. Surprisingly, the bulk modulus B_0 of the high pressure phase is much lower than that of the low pressure phase after the incorporation of the minor phase: 121.6 (±10.6) GPa for the low pressure phase and 92.1 (10.5) GPa for the high pressure phase. Although there are some discrepancies between calculated B_0 and experimental B_0,[30,33,34] it may be due to the difference in the practical solidification process and exchange-correlation approximation adopted in the calculation. In our work, after dissolving the minor phase under pressure, B_0 of the high pressure phase is nearly the same as that of pure TiZrHfNb HEA, 88.3 (±13.5) GPa experimentally reported in the literature,[31] which further demonstrated that the merged high pressure phase was the pure BCC phase. Due to the limited capability of the hydrostatic pressure of silicone oil, the volume change of the minor phase irregularly decreased from about 15 GPa. Meanwhile, the low diffraction intensity from the minor phase gave large uncertainties, and only the unit cell volume is shown in Fig. 3(b). The volume decreased almost linearly against pressure below 10.5 GPa, and the linearity was lost above 10.5 GPa.

At low pressure, the main phase has much larger B_0, i.e., more incompressible, while the merged high pressure phase shows a much more compressible property. This is quite different from the regular structure phase transition. Under pressure, materials turn to a higher density structure. Phase transition usually turns materials into a more incompressible phase. Here, with the aid of pressure, the starting TiZrHfNb BCC HEA with 1% minor phase turns to a more compressible uniform single BCC phase. From the EOS fitting result, it is found that the V_o value (unit cell volume at ambient pressure) of the high pressure phase is even larger than V_o of the low pressure phase, which was further confirmed by the decompression measurements with a larger unit cell volume, as shown in Fig. 3(a). This indicated that high pressure processing can effectively tune and quench the mechanical properties of HEA by altering the phase constitution.

Remarkably, the compressibility of HEA was largely affected by the minor composition variation, which implied a strong interaction between the main phase and the minor phase during compression. Figures 3(a) and 3(b) show ~21% unit cell volume difference between two phases at the ambient pressure. From 1.8 GPa to 10.5 GPa, the main phase dropped 5.6% in volume, but the minor phase only dropped 2.6%. The huge difference in volume shrinkage would inevitably induce a large lattice distortion and hence higher interfacial energy between these two phases. This is confirmed by the following strain analysis based on Scherrer's equation. The first five diffraction peak widths from the main phase during compression were fit into the following equation:[33–37]

$$FWHM^2 \cos^2\theta = \left(\frac{\lambda}{d}\right)^2 + \sigma^2 \sin^2\theta,$$

where FWHM is the full-width at half-maximum of the diffraction peak on the 2θ-scale. The symbols d, λ, σ, and θ denote the grain size, x-ray wavelength, lattice distortion or strain, and diffraction angle, respectively. Figures 4(a) and 4(b) illustrate the evolutions of FWHMs from the first 5 peaks and strain for the entire compression data of the main phase.

While increasing pressure, the associated FWHM and strain values show local minima at around 13.2 GPa, 36 GPa, and 56.3 GPa.

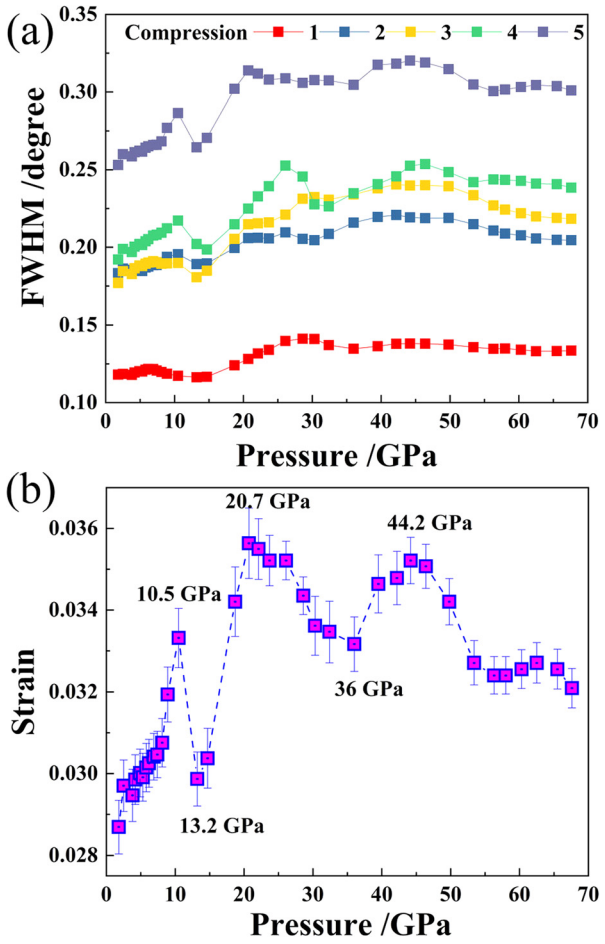

FIG. 4. (a) FWHMs of the first five diffraction peaks vs pressure for the main phase; (b) lattice strain evolution in the main phase during compression.

At the first pressure point, the strain value holds the lowest record as the local interface distortion between two phases was annealed during the high temperature synthesis. From the XRD results discussed above, in the pressure range from ambient to 10.5 GPa, due to the quite different compressibility between minor and main phases, the local balance formed in the as-cast form at the interface will be distorted larger as pressure increases. This causes the lattice strain to increase monotonically in this first increasing stage (1.8–10.5 GPa range). Unlike monotonic softening or hardening behavior in regular tensile/compression tests,[32] microscopic strain in this work showed abrupt softening behavior at 13.2 GPa. It is well known that the mechanical properties and phase transition mechanism of materials are closely associated with the presence of the minor phase and the interfacial boundary between two phases.[38] As shown in Fig. 3(b), the unit cell volume of the minor phase evidently deviated away from its normal compression curve. When the "merging process" proceeded along with increasing interaction between two phases, the main phase cannot withstand the internal lattice distortion until the softening behavior occurred. Therefore, the abnormal softening behavior for the main phase at 13.2 GPa was attributed to the unusual unit cell volume change of the second phase. The continuous increase in the mismatch in the unit cell volume between two phases promoted the development of lattice distortion. As the unit cell volume deviation of the minor phase increased, the lattice strain reached the maximum at about 20.7 GPa. Starting from 20.7 GPa, the volume amount of the minor phase started to decrease sharply, which reduced the interfacial volume and caused the reduction of strain in the main phase. Beyond 30 GPa, it is hard to fit the diffraction peak of the minor phase shown in Fig. 1(a). After 36 GPa, HEA has completely become a single BCC phase structure confirmed by the two-dimensional XRD patterns. From strain evolution, it is also found that the complete merging of the two phases occurred around 36 GPa, which corresponds to the minimum of strain. Upon further compression, pressure-induced lattice distortion resumed up to 44.2 GPa, during which the highly stressed zone possibly formed due to the limited hydrostatic pressure condition. When this high pressure single-phase HEA cannot withstand the internal strain anymore, the plastic deformation occurred to relax the strain energy and further led to the decrease in lattice strain after 44.2 GPa. Thus, the starting alloy as a mixture of main and minor phases with a small deviation in the composition has much higher incompressibility due to the large interface strain between two phases, which provides the "pinning-in" effect from plastic deformation. Under high pressure, the minor phase can be "dissolved" into the matrix by the interface interaction, and thus, the HEA loses the micro-interfacial barriers and becomes a uniform solid solution with a more compressible behavior.

Although HEA tends to form a single-phase solid solution, minor composition fluctuation was unavoidable in the as-cast matrix due to chemical complexity.[14,39] The resulted mismatch of the lattice parameter is the fundamental origin of strain energy in HEA along with the presence of lattice distortion.[40] It has been confirmed that this internal strain can result in the modification of the material mechanical properties and phase transition process.[17,33–36,41,42] Based on the geometric model of atomic size, atomic fraction, and packing density, a limiting case of crystalline-amorphous transition will take place when the residual strain is more than 10% in MPEA.[43] Therefore, it is possible to form high entropy metallic glass by modulating lattice distortion of high entropy crystalline alloy. High pressure can be used as a powerful tool to tune the lattice distortion or even atom structure and finally change the mechanical properties of HEA.

In summary, *in situ* high pressure-synchrotron x-ray diffraction revealed diverse mechanical behaviors in dual-phase TiZrHfNb HEA. Upon compression, the two starting highly incompressible phases merged into a single-phase with a much lower bulk modulus that is close to that of homogeneous single-phase TiZrHfNb HEA. This is unlike most single-phase alloys, as the high pressure induced phase transition usually leads to a higher bulk modulus phase. In this work, the high pressure phase can be recovered to ambient conditions. This abnormal compression behavior demonstrates that the mechanical properties of HEA can be remarkably affected by the minor composition fluctuation in HEA. Pressure can be applied as a powerful tool to unify the two phases to a single one and tune the compressibility in large.

See the supplementary material for the sample preparation method, microstructure and chemistry characterization of the sample, and the details of *in situ* high-pressure synchrotron XRD.

K.Z. and S.P. contributed equally to this work.

This work was supported by the National Nature Science Foundation of China under Grants Nos. 11804010, U1530402, and 51527801, China Postdoctoral Science Fund (Grant No. 2016M600909), and China sponsorship council. The beamline 13-ID-D (GeoSoilEnviroCARS) was supported by the National Science Foundation (NSF)-Earth Sciences (No. EAR-1634415) and Department of Energy (DOE)-GeoSciences (No. DE-FG02-94ER14466). The Advanced Photon Source was supported by DOE-BES, under Contract No. DE-AC02-06CH11357.

REFERENCES

[1]J. W. Yeh, S. K. Chen, S. J. Lin, J. Y. Gan, T. S. Chin, T. T. Shun, C. H. Tsau, and S. Y. Chang, Adv. Eng. Mater. **6**, 299–303 (2004).
[2]B. Gludovatz, A. Hohenwarter, D. Catoor, E. H. Chang, E. P. George, and R. O. Ritchie, Science **345**, 1153–1158 (2014).
[3]P. Kozelj, S. Vrtnik, A. Jelen, S. Jazbec, Z. Jaglicic, S. Maiti, M. Feuerbacher, W. Steurer, and J. Dolinsek, Phys. Rev. Lett. **113**, 107001 (2014).
[4]Y. Zhang, T. T. Zuo, Z. Tang, M. C. Gao, K. A. Dahmen, P. K. Liaw, and Z. P. Lu, Prog. Mater. Sci. **61**, 1–93 (2014).
[5]Z. Li, K. G. Pradeep, Y. Deng, D. Raabe, and C. C. Tasan, Nature **534**, 227–230 (2016).
[6]Z. Lei, X. Liu, Y. Wu, H. Wang, S. Jiang, S. Wang, X. Hui, Y. Wu, B. Gault, P. Kontis, D. Raabe, L. Gu, Q. Zhang, H. Chen, H. Wang, J. Liu, K. An, Q. Zeng, T. G. Nieh, and Z. Lu, Nature **563**, 546–550 (2018).
[7]J. Guo, H. Wang, F. von Rohr, Z. Wang, S. Cai, Y. Zhou, K. Yang, A. Li, S. Jiang, Q. Wu, R. J. Cava, and L. Sun, Proc. Natl. Acad. Sci. U. S. A. **114**, 13144–13147 (2017).
[8]F. Otto, Y. Yang, H. Bei, and E. P. George, Acta Mater. **61**, 2628–2638 (2013).
[9]B. Cantor, I. T. H. Chang, P. Knight, and A. J. B. Vincent, Mater. Sci. Eng.: A **375–377**, 213–218 (2004).
[10]O. Senkov, G. Wilks, J. Scott, and D. Miracle, Intermetallics **19**, 698–706 (2011).
[11]Y. F. Ye, Q. Wang, J. Lu, C. T. Liu, and Y. Yang, Mater. Today **19**, 349–362 (2016).
[12]Y. J. Liang, L. Wang, Y. Wen, B. Cheng, Q. Wu, T. Cao, Q. Xiao, Y. Xue, G. Sha, Y. Wang, Y. Ren, X. Li, L. Wang, F. Wang, and H. Cai, Nat Commun. **9**, 4063 (2018).
[13]Z. Fu, L. Jiang, J. L. Wardini, B. E. MacDonald, H. Wen, W. Xiong, D. Zhang, Y. Zhou, T. J. Rupert, and W. Chen, Sci. Adv. **4**, eaat8712 (2018).
[14]H. Huang, Y. Wu, J. He, H. Wang, X. Liu, K. An, W. Wu, and Z. Lu, Adv. Mater. **29**, 1701678 (2017).
[15]B. Schuh, B. Völker, J. Todt, N. Schell, L. Perrière, J. Li, J. P. Couzinié, and A. Hohenwarter, Acta Mater. **142**, 201–212 (2018).
[16]J. Y. He, W. H. Liu, H. Wang, Y. Wu, X. J. Liu, T. G. Nieh, and Z. P. Lu, Acta Mater. **62**, 105–113 (2014).
[17]Y. J. Zhou, Y. Zhang, F. J. Wang, and G. L. Chen, Appl. Phys. Lett. **92**, 241917 (2008).
[18]L. R. Owen, E. J. Pickering, H. Y. Playford, H. J. Stone, M. G. Tucker, and N. G. Jones, Acta Mater. **122**, 11–18 (2017).
[19]F. X. Zhang, S. Zhao, K. Jin, H. Xue, G. Velisa, H. Bei, R. Huang, J. Y. P. Ko, D. C. Pagan, J. C. Neuefeind, W. J. Weber, and Y. Zhang, Phys. Rev. Lett. **118**, 205501 (2017).
[20]J.-W. Yeh, S.-Y. Chang, Y.-D. Hong, S.-K. Chen, and S.-J. Lin, Mater. Chem. Phys. **103**, 41–46 (2007).
[21]Q. He and Y. Yang, Front. Mater. **5**, 42 (2018).
[22]Y. Tong, S. Zhao, H. Bei, T. Egami, Y. Zhang, and F. Zhang, Acta Mater. **183**, 172–181 (2020).
[23]Y. Zou, S. Maiti, W. Steurer, and R. Spolenak, Acta Mater. **65**, 85–97 (2014).
[24]W. Guo, W. Dmowski, J.-Y. Noh, P. Rack, P. K. Liaw, and T. Egami, Metall. Mater. Trans. A **44**, 1994–1997 (2013).
[25]L. Zhang, Y. Wang, J. Lv, and Y. Ma, Nat. Rev. Mater. **2**, 17005 (2017).
[26]H. W. Sheng, H. Z. Liu, Y. Q. Cheng, J. Wen, P. L. Lee, W. K. Luo, S. D. Shastri, and E. Ma, Nat. Mater. **6**, 192–197 (2007).
[27]F. Zhang, Y. Wu, H. Lou, Z. Zeng, V. B. Prakapenka, E. Greenberg, Y. Ren, J. Yan, J. S. Okasinski, X. Liu, Y. Liu, Q. Zeng, and Z. Lu, Nat. Commun. **8**, 15687 (2017).
[28]F. X. Zhang, S. Zhao, K. Jin, H. Bei, D. Popov, C. Park, J. C. Neuefeind, W. J. Weber, and Y. Zhang, Appl. Phys. Lett. **110**, 011902 (2017).
[29]C. L. Tracy, S. Park, D. R. Rittman, S. J. Zinkle, H. Bei, M. Lang, R. C. Ewing, and W. L. Mao, Nat. Commun. **8**, 15634 (2017).
[30]H. Song, F. Tian, Q.-M. Hu, L. Vitos, Y. Wang, J. Shen, and N. Chen, Phys. Rev. Mater. **1**, 023404 (2017).
[31]A. S. Ahmad, Y. Su, S. Y. Liu, K. Ståhl, Y. D. Wu, X. D. Hui, U. Ruett, O. Gutowski, K. Glazyrin, H. P. Liermann, H. Franz, H. Wang, X. D. Wang, Q. P. Cao, D. X. Zhang, and J. Z. Jiang, J. Appl. Phys. **121**, 235901 (2017).
[32]F. Birch, J. Geophys. Res. **57**, 227–286, https://doi.org/10.1029/JZ057i002p00227 (1952).
[33]X. Yan, H. Dong, G. Sun, X. Ren, D. He, and W. Yang, Phys. Rev. B **94**, 144104 (2016).
[34]X. Yan, H. Dong, Y. Li, C. Lin, C. Park, D. He, and W. Yang, Sci. Rep. **6**, 24958 (2016).
[35]X. Yan, D. Tan, X. Ren, W. Yang, D. He, and H.-K. Mao, Appl. Phys. Lett. **106**, 171902 (2015).
[36]Q. Hu, L. Lei, X. Yan, L. Zhang, X. Li, F. Peng, and D. He, Appl. Phys. Lett. **109**, 071903 (2016).
[37]A. Singh, A. Jain, H. Liermann, and S. Saxena, J. Phys. Chem. Solids **67**, 2197–2202 (2006).
[38]L. Ma, L. Wang, Z. Nie, F. Wang, Y. Xue, J. Zhou, T. Cao, Y. Wang, and Y. Ren, Acta Mater. **128**, 12–21 (2017).
[39]Y. Ma, Q. Wang, C. Li, L. J. Santodonato, M. Feygenson, C. Dong, and P. K. Liaw, Scr. Mater. **144**, 64–68 (2018).
[40]Y. F. Ye, Y. H. Zhang, Q. F. He, Y. Zhuang, S. Wang, S. Q. Shi, A. Hu, J. Fan, and Y. Yang, Acta Mater. **150**, 182–194 (2018).
[41]C. Wang, C. L. Tracy, S. Park, J. Liu, F. Ke, F. Zhang, T. Yang, S. Xia, C. Li, Y. Wang, Y. Zhang, W. L. Mao, and R. C. Ewing, Appl. Phys. Lett. **114**, 091902 (2019).
[42]B. Cheng, F. Zhang, H. Lou, X. Chen, P. K. Liaw, J. Yan, Z. Zeng, Y. Ding, and Q. Zeng, Scr. Mater. **161**, 88–92 (2019).
[43]Y. F. Ye, C. T. Liu, and Y. Yang, Acta Mater. **94**, 152–161 (2015).